Mon. Not. R. Astron. Soc. **372,** 53–59 (2006) doi:10.1111/j.1365-2966.2006.10708.x

Detecting a rotation in the ϵ Eridani debris disc

C. J. Poulton,★ J. S. Greaves and A. C. Cameron
School of Physics and Astronomy, University of St. Andrews, North Haugh, St. Andrews, Fife KY16 9SS

Accepted 2006 June 2. Received 2006 June 1; in original form 2006 March 7

ABSTRACT

The evidence for a rotation of the ϵ Eridani debris disc is examined. Data at 850-μm wavelength were previously obtained using the Submillimetre Common User Bolometer Array (SCUBA) over periods of 1997–1998 and 2000–2002. By χ^2 fitting after shift and rotation operations, images from these two epochs were compared to recover proper motion and orbital motion of the disc. The same procedures were then performed on simulated images to estimate the accuracy of the results.

Minima in the χ^2 plots indicate a motion of the disc of approximately 0.6 arcsec per year in the direction of the star's proper motion. This underestimates the true value of 1 arcsec per year, implying that some of the structure in the disc region is not associated with ϵ Eridani, originating instead from background galaxies. From the χ^2 fitting for orbital motion, a counterclockwise rotation rate of $\sim 2\overset{\circ}{.}75$ per year is deduced. Comparisons with simulated data in which the disc is not rotating show that noise and background galaxies result in approximately Gaussian fluctuations with a standard deviation of $\pm 1\overset{\circ}{.}5$ per year. Thus, counterclockwise rotation of disc features is supported at approximately a 2σ level, after a 4-yr time difference. This rate is faster than the Keplerian rate of $0\overset{\circ}{.}65$ per year for features at $\approx$65 au from the star, suggesting their motion is tracking a planet inside the dust ring.

Future observations with SCUBA-2 can rule out no rotation of the ϵ Eridani dust clumps with $\sim 4\sigma$ confidence. Assuming a rate of about $2\overset{\circ}{.}75$ per year, the rotation of the features after a 10-yr period could be shown to be $\geqslant 1^\circ$ per year at the 3σ level.

Key words: Kuiper Belt – circumstellar matter – planetary systems: formation – planetary systems: protoplanetary discs – submillimetre.

1 INTRODUCTION

1.1 ϵ Eridani: a special case

Debris discs around nearby stars represent extra-solar analogues of the Kuiper Belt. It is in this context that studying the ϵ Eridani dust ring is of particular interest since it is of spectral type K2V, not too dissimilar to the Sun, but with a much younger age of 0.8 Gyr (Song et al. 2000; Di Folco et al. 2004) and thus represents an analogue to the young Solar system. It is generally thought that protoplanetary discs evolve into debris discs after planets have formed, a process that is completed within 10–100 Myr after star birth (Holland et al. 1998; Schutz et al. 2004). Greaves et al. (2004) have noted that there is an apparent lack of overlap between stars with debris discs detectable at submillimetre wavelengths and those with radial velocity planet detections. There are only a few stars with positive detections for both an infrared (IR) dust excess and a radial velocity planet (Dominik et al. 1998; Beichman et al. 2005). While this is likely to reflect the small number of stars searched for both phenomena, ϵ Eridani remains unique in having resolved structure within the debris ring (Greaves et al. 1998, 2005) plus an inner gas giant planet detected by Doppler wobble (Hatzes et al. 2000). Further evidence for this planet comes from the forced offset of the centre of the ring (Greaves et al. 2005), consistent with a forced eccentricity of the dust particles (Wyatt et al. 1999). The ring structure also appears perturbed as if by a more distant gas giant, but this body has not yet been imaged, with a maximum mass constraint at around the dust ring radius of approximately 5 M_J (Macintosh et al. 2003).

1.2 Planet hunting by tracking of disc features

An IR excess around ϵ Eridani was first detected during photometric measurements by the *Infrared Astronomical Satellite* (*IRAS*) (Aumann 1988), soon after the initial discovery of an IR excess around Vega (Aumann et al. 1984). Subsequent submillimetre observations at 850 μm with the Submillimetre Common User Bolometer Array (SCUBA) by Greaves et al. (1998) resolved the disc and showed a ring-like structure. The faint ring surrounding ϵ Eridani has not yet been successfully imaged at optical wavelengths (Proffitt et al. 2004).

★E-mail: cp85@st-and.ac.uk (CJP)

Further SCUBA observations made in 2000–2002 (Greaves et al. 2005) allow us to study the motions of the substructure in the ring over a 5-yr period. If clump features are tracking the orbital motion of a planet within the ring, they should appear to rotate faster than the Keplerian rate at the ring radius; this would be an unambiguous signature of a planet with the forced period providing a measure of its orbital semimajor axis. Clumps will appear in a disc where planet formation has taken place because the planets will migrate outwards via angular momentum exchange with the remaining planetesimals. As the planets migrate outwards, the associated gravitational resonances also move out, thus trapping dust particles outside the planet's orbit into mean motion resonances (Wyatt et al. 1999, 2003). The Kuiper Belt in the Solar system probably formed in a similar way, where the material is thought to have been pushed outwards by a mean motion resonance associated with Neptune as it migrated further away from the Sun (Malhotra 1995; Gomes 2003; Levison & Morbidelli 2003).

Circumstellar dust, trapped into resonances by an outwardly migrating planet (Wyatt et al. 1999; Quillen & Thorndike 2002; Wyatt et al. 2003), is expected to be observable at submillimetre wavelengths. Whilst the Vega and Fomalhaut disc asymmetries have been modelled (Wyatt et al. 2003; Wyatt & Dent 2002), the ϵ Eridani dust ring offers a unique prospect to directly track motion of clumps over time, because of its favourable inclination ($\sim 25^\circ$ from face-on to the observer) and the fact that this is one of the closest stars to the Sun at a distance of 3.22 pc. Models of the distribution of the ϵ Eridani clumps (Ozernoy et al. 2000; Quillen & Thorndike 2002) suggest the perturbing planet lies $\approx$40–60 au from the star, thus the clumps are expected to orbit with a period of $\approx$280–520 yr. These rotation rates of $0\overset{\circ}{.}7$–$1\overset{\circ}{.}3$ per year, corresponding to particular resonant periods (Ozernoy et al. 2000; Quillen & Thorndike 2002), require long times to detect. Here, we present a preliminary analysis over 5 yr of data, making use of image fitting to statistically recover any small rotation present.

2 OBSERVATIONS

The results used here consist of the 5 yr data set presented by Greaves et al. (2005). Observations of ϵ Eridani at 850 μm were made with SCUBA between 1997 August and 2002 December, in total comprising 56 images and an integration time of 33.5 h. The data set is split into two parts, one including data taken during 1997–1998 and the other from 2000 to 2002; the observing runs were bunched in time so that the effective mid-points of the two periods are around 4 yr apart. The 2000–2002 data set has a noise level lower by a factor of 2, as a result of longer duration and better sensitivity. Data were also obtained at 450 μm, but the SCUBA filter used in 1997–1998 had a low throughput, and so this image cannot be used for time-dependent studies.

The analysis made here is of the co-added 1997–1998 data compared to the co-added 2000–2002 results. The stellar proper motion is −1 arcsec in RA per year, so any disc emission associated with the star should shift by approximately 4 arcsec west, with some blurring because the observing periods were spread out. The diffraction-limited full width at half-maximum (FWHM) beam size at 850 μm was 15×15.5 arcsec^2, but the data have been smoothed using a 7 arcsec Gaussian to an effective 17 arcsec beam (Greaves et al. 2005). The net pointing errors are expected to be small, below the level of the 1 arcsec cell size in the images. The noise for the 1997–1998 data set is 4.3×10^{-3} mJy arcsec^{-2} (0.96 mJy beam^{-1}) with 2.4×10^{-3} mJy arcsec^{-2} (0.54 mJy beam^{-1}) for the 2000–2002 data set. Photospheric emission of 1.7 ± 0.2 mJy has been subtracted from the images, for ease of comparison with simulations that neglect the star.

3 SIMULATED DATA

The proper motion and rotation of dust features associated with the star can be assessed by translating and rotating the 1997–1998 and 2000–2002 co-added images to find the best match. The accuracy of the results was evaluated by comparison with simulated data with comparable noise, background galaxies and a foreground consisting of clumps embedded in a smooth ring of radius 20 arcsec centred on the star.

Each simulated image was constructed from a set of frames, each representing an individual observation taken with SCUBA. The simulated analogue of the 1997–1998 data set comprised 22 frames of equal depth, which when co-added reproduced the noise in the actual data at the final 17-arcsec resolution. The range of proper motion offset compared to the last real data taken was 4–5 arcsec. A similar procedure was followed to simulate the 2000–2002 data, using 34 frames and a proper motion range of 0–2.5 arcsec. The difference in depths between the real 1997–1998 and 2000–2002 data sets was accounted for by both the number of images in each simulated data set and the noise levels that were input into each set. While the number of input frames is the real value, the equal noise value per frame is a simplification (as it was too complex to simulate the duration and observing conditions of every real frame). Thus, the effective mid-points of the two observing periods, about 4 yr apart, may not be exactly matched in the simulated results.

Each simulated frame representing an observation by SCUBA was constructed from random noise, random background galaxies and a foreground (ring and clumps embedded in the ring) of comparable brightness to the observed data. The same background galaxies were used in both the 1997–1998 and 2000–2002 frames but a different sample generated for each simulation. The chopping motion of the secondary mirror of the telescope used to determine sky levels was also simulated. All of these effects contribute to the real images; the data should thus represent one possible outcome of the simulations, to within the accuracy of the simplifications used.

3.1 Simulation details

The noise image was made by choosing the flux for each individual pixel randomly from a Gaussian distribution and then smoothing spatially with a 7 arcsec Gaussian as was done for the observed data. This assumes the noise per 1 arcsec pixel is statistically independent. The mean for the noise distribution was zero and the σ value was chosen so that the final simulated images had a standard deviation of flux per beam matching the real data set once the galaxy population had been added.

The integral galaxy counts $N(>S)$ for each flux, S, at 850 μm were modelled with Poisson statistics using numbers from Barnard et al. (2004), by a double power law given by

$$N(>S) \propto S^{-\alpha} \tag{1}$$

with $\alpha = 0.94$ for $S < 1.18$ mJy and $\alpha = 2$ for $S \geqslant 1.18$ mJy. Each galaxy's point-like flux was smoothed with a two-dimensional Gaussian to reflect the size of the beam of the James Clerk Maxwell Telescope (JCMT) at 850 μm and then placed at random coordinates chosen from a uniform distribution. Thus, no area of the image was favoured and any possible galaxy clustering was neglected.

The foreground was modelled by adding beam-sized two-dimensional Gaussian regions of flux to a ring. The ring was created

by placing Gaussians at every pixel at distances between 17.5 and 22.5 arcsec from the star, producing an annulus centred on the star with the radius and width observed (Greaves et al. 2005). The flux per pixel in the ring was chosen to match the smooth level observed (i.e. between clumps) of $\approx 10^{-2}$ mJy arcsec^{-2}. Greaves et al. (2005) identified three clumps with possible rotation located at northeast, northwest and southeast of the star at a radius of 20 arcsec, and thus three clumps were added at these positions in the simulated ring. The peak fluxes of the clumps were set at $\approx 1.5 \times 10^{-2}$ mJy arcsec^{-2} so that the total foreground had peak fluxes at the clump locations of $\approx 2.5 \times 10^{-2}$ mJy arcsec^{-2}. This is the mean of the total fluxes towards the three candidate moving clumps in the observed data (Greaves et al. 2005).

Proper motion of the disc was simulated by translating the foreground relative to the background for each of the simulated observations, by a distance corresponding to the epochs of individual real frames. In the observed data, a correction for the annual proper motion of ϵ Eridani ($\mu_\alpha = -0.976$ arcsec yr^{-1}, $\mu_\delta = 0.018$ arcsec yr^{-1}) (ESA 1997) was made by sorting and shifting the frames to a precision of 0.5 arcsec bins in RA only (Greaves et al. 2005). This correction was also performed on the simulated observations, and so the background galaxies (fixed with respect to the sky) will appear to move at the rate of the proper motion but towards positive RA, in a co-ordinate frame comoving with the star.

Also simulated was the chopping procedure performed by the JCMT, used to remove sky fluctuations. 'Blank' regions of sky on either side of the field of interest are observed interleaved with the on-source observations, and subtracted to leave only astronomical signal; for comments on the limitations see Archibald et al. (2002). If background galaxies lie within the SCUBA field of view at either off-source position, 'holes' with magnitude equal to half the brightness of the galaxies being chopped on to will appear in the final observed image. Due to variations in the chop direction, such holes will be blurred in the on-source residual frame and thus difficult to recognize. As chopping introduces extra fluctuations and modifies the background galaxy contributions, it was important to include it in the simulations.

The noise, background galaxies and foreground images were constructed for a 400 × 400 pixel square frame but the field of view of SCUBA on the JCMT is roughly circular with a radius of 72 arcsec. It was necessary to simulate this larger area of sky to allow the chopping procedure to be simulated. Flux values for each pixel within an area of sky were read into two-dimensional arrays at the position of the source, M, and the two off-source positions to the left, L, and right, R, of the source. The pixel fluxes used in the final images, I, were then calculated using

$$\mathrm{I}(x, y) = \mathrm{M}(x, y) - \frac{[\mathrm{L}(x, y) + \mathrm{R}(x, y)]}{2}. \quad (2)$$

Chopping in azimuth was used for the real data, so that the left and right chop throws fell on different sky regions depending on the source elevation. This was accounted for in the simulations by varying the angle between the chop throw and the line of constant right ascension (horizontal in the images) randomly between -50° and 50°. In the observations, chop throws of 80 arcsec (5 per cent of images), 100 arcsec (55 per cent) and 120 arcsec (40 per cent) were used. A chop throw of 120 arcsec was used for all of the simulated chopping.

Some small effects were neglected in the simulations. The disc is fairly close to face-on to the observer, but inclined at $\sim 25^\circ$ from the sky plane and so actually appears as an ellipse in the sky. Assuming a rotation rate of 2.°75 per year, a clump moving along the direction of the minor axis of the ellipse will have a motion that is only $\sim$0.3 arcsec less than a clump moving parallel to the direction of the major axis. Therefore, it was reasonable to approximate the ring as circular to simplify the rotation of the foreground image. The annual shifts in position due to parallax for ϵ Eridani are $\pm$0.3 arcsec and these were neither accounted for in the telescope tracking software nor included in the modelling. In the observed data, 68 per cent of the images co-added were taken between August and October and so the effect of smearing due to parallax errors will be less than 0.3 arcsec. The dust ring was also simulated as being centred on the star, neglecting the offset of 1.5–2 arcsec identified by Greaves et al. (2005) and suspected to be forced by the inner planet. We assume the bulk motions of the clumps still follow circular orbits.

3.2 Simulation output

The real images are shown in Fig. 1 and examples of the simulated images are shown in Fig. 2. The simulated images recreate a ring with comparable brightness, size and morphology to that seen in the observations. The regions surrounding the ring also show comparable levels of noise and density of background objects. Differences

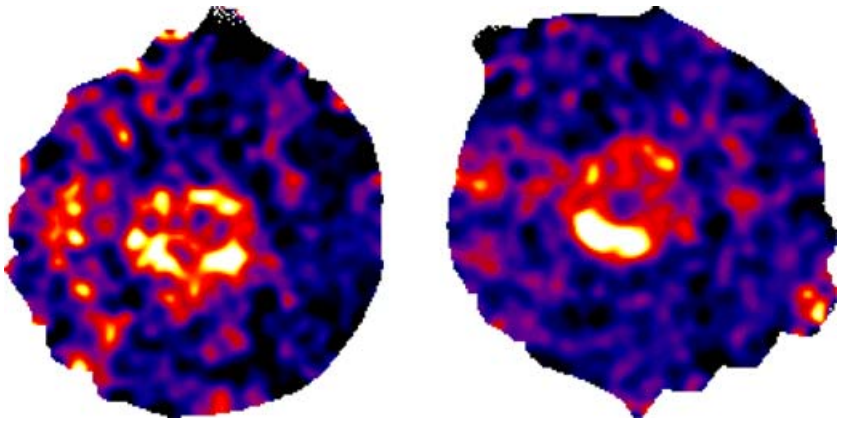

Figure 1. Observations of the ϵ Eridani debris disc taken with SCUBA on the JCMT. Left-hand side: 1997–1998 data set (averaged over 22 images) in a 1-arcsec pixel grid in RA, Dec. coordinates (north is up, east is left), plotted with the dynamic ranges min $= -1 \times 10^{-2}$, max $= 2.5 \times 10^{-2}$ mJy arcsec^{-2}. Right-hand side: 2000–2002 data set (averaged over 34 images) with the same parameters.

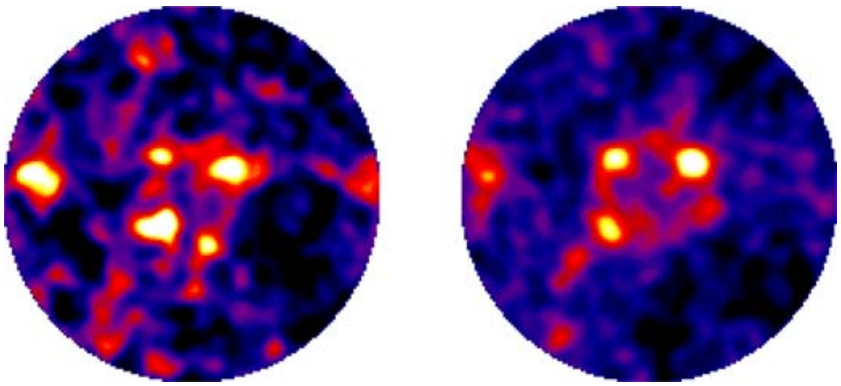

Figure 2. As for Fig. 1 but for simulated SCUBA images with no rotation of the foreground clumps: (left-hand side) example of simulated 1997–1998 image, (right-hand side) the corresponding 2000–2002 image. Other parameters are as in Fig. 1.

between the two simulated images are at a similar level to those in the real data of Fig. 1. Although the image structure looks complex, this is in part because the false-colour scale both includes a wide flux range (negative as well as positive signals) and also tends to enhance features with low levels of contrast, as discussed by Greaves et al. (2005).

The simulation procedure was also repeated to resemble a future observation that could be taken in 2007 with SCUBA-2 – a replacement camera for SCUBA with greater sensitivity, fidelity and field of view (Holland et al. 2003; Audley et al. 2004). For this simulation, the noise was set to zero as it will fall below the background confusion in an observation of only ∼1 h. The chopping part of the simulated data algorithms was also disabled since SCUBA-2 will sample rapidly enough that sky fluctuations will be negligible and so chopping will not be required. (Chopping can be re-introduced in the data analysis where necessary for matching SCUBA-2 images of ϵ Eridani with those already taken with SCUBA.) Any candidate rotation of the disc identified here can thus be checked by extending the total timeline of observations to 10 yr (from 1997 to 2007).

4 DETECTING A ROTATION

The simplest method of measuring rotation would be to track individually identified clumps. However, clump extraction algorithms (Williams et al. 1994; Bertin & Arnouts 1996) are not well adapted to finding clumps and arcs within a ring. Hence, a χ^2-fitting technique was adopted instead, with the advantage of using all the information in the image simultaneously. The χ^2 per pixel value for two images, I_1 and I_2, with measured noise σ_1 and σ_2, using only pixels in a box with its lower left and upper right corners defined by (x,y) cartesian co-ordinates (a_1, b_1) and (a_2, b_2), can be calculated using

$$\chi^2 = \frac{\sum_{x=a_1}^{a_2} \sum_{y=b_1}^{b_2} [I_1(x, y) - I_2(x, y)]^2}{(a_2 - a_1 + 1)(b_2 - b_1 + 1)\left(\sigma_1^2 + \sigma_2^2\right)}. \quad (3)$$

The χ^2 per pixel values between the 2000–2002 data set and the 1997–1998 data set were calculated as the 1997–1998 data set was shifted in right ascension and rotated relative to the 2000–2002 data set, using the tasks 'SLIDE' and 'ROTATE' in the KAPPA software package (Currie & Berry 2004). The minima in plots of χ^2 per pixel as a function of right ascension shift or rotation angle then identified the best solutions for each (independently). The region of the image included in the χ^2 fit was defined by a 70 arcsec-square box, as this included all of the disc with as little off-source background as possible; extra background galaxies included in a larger box tend to cause the χ^2 fits to incorrectly favour a shift and rotation of zero.

For the simulated SCUBA-2 observation, the χ^2 per pixel values were calculated twice, once for the future 2007 observation compared to the 1997–1998 SCUBA data set, and again for 2007 compared to the 2000–2002 SCUBA data. The two χ^2 values corresponding to the same shift or rotation rate were then averaged to create the final χ^2 per pixel curves. We also performed simulations with no galaxies or noise, and verified that the true rotation values were recovered correctly.

There are three possible ways in which the regions of emission in the ring may be behaving.

(i) The ring consists of only background galaxies and therefore the features are not tracking with the proper motion of the star or revolving around the star's position.

(ii) The ring features are tracking with the proper motion of the star but are revolving around the star at the Keplerian period of the ring which would not require a planet to explain the motion.

(iii) The ring features are tracking with the proper motion of the star and revolving around the star at the period of a planet at tens of au.

To establish which of these explanations gives the best description of the data, the observed data were fitted for the proper motion of emission in the disc region, and then fitted to establish a rotation rate of the ring features. Then for comparison, 100 sets of simulated data were made with no proper motion or rotation of the foreground to quantify the random fluctuations due to noise, background galaxies and chopping on to background galaxies. This was then repeated but assuming the foreground was tracking with the proper motion of the star and with the foreground rotated at rates of 0° (i.e. no rotation), 1°, 2°, 4° and 10° per year (unrealistically large but included for comparison). The purpose of trying different rotation rates was to examine how well the true rate is recovered, given that non-moving background galaxies introduce a bias towards a χ^2 minimum around zero degrees.

5 RESULTS AND DISCUSSION

Fig. 3 shows χ^2 per pixel as a function of the annual proper motion and rotation rate of the 1997–1998 image relative to the 2000–2002 data. Five examples of simulations are shown for comparison. Table 1 lists the statistics from the full sets of simulations, each set comprising 100 comparisons of pairs of images.

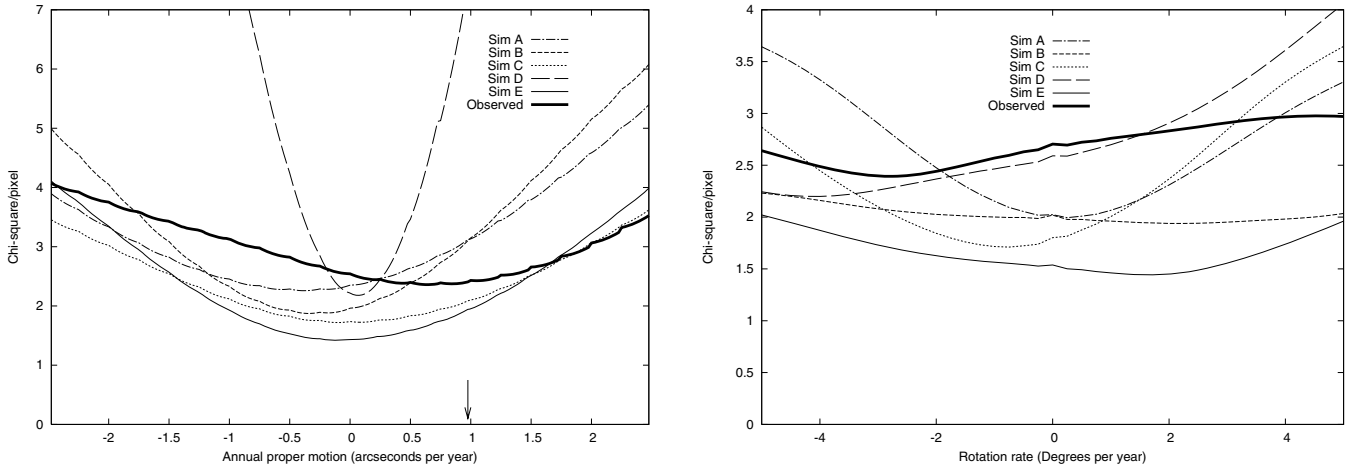

Figure 3. χ^2 per pixel curves for observed data and simulations. Left-hand side: fits for annual proper motion shift from the 1997–1998 to the 2000–2002 data set. Thick curve shows observed data; other curves are five random simulations with no proper motion or rotation. Positive shifts are to the right-hand side (−ve in RA) and the arrow indicates the known proper motion of ϵ Eridani ($\mu_\alpha = -0.976$ arcsec yr^{-1}). Small deviations in the curves are caused by slight imperfections in the linear interpolation. The narrow curve (Sim D) originates from a very bright galaxy in the ring, forcing a minimum that must be close to zero. Right-hand side: fits for annual rotation rates, comparing 1997–1998 and 2000–2002 data sets and with corrections made for proper motion. Thick curve shows observed data; thin curves are five random simulation pairs with proper motion corrections included but no rotation.

Table 1. Proper motion shifts and rotations recovered from χ^2 fitting of six simulated SCUBA data sets each consisting of 100 simulated 1997–1998 and 2000–2002 images with foreground, background galaxies, noise and chopping included.

Simulation set no.	Simulated motion[a] (arcsec yr^{-1})	Average motion (arcsec yr^{-1})	Motion σ (arcsec yr^{-1})	Simulated rotation ($^\circ$ yr^{-1})	Average rotation ($^\circ$ yr^{-1})	Rotation σ ($^\circ$ yr^{-1})	5σ Clipping results (no. excluded)	Average min χ^2 value
1	0	0.01	±0.28	0	−0.03	±1.23	5	1.92
2	+1	0.79	±0.38	0	−0.15	±1.58	4	2.03
3	+1	0.78	±0.42	−1	−0.68	±1.83	5	2.03
4	+1	0.73	±0.44	−2	−0.96	±1.87	2	2.06
5	+1	0.65	±0.47	−4	−1.92	±2.55	7[b]	2.14
6	+1	0.63	±0.47	−10	−4.83	±13.71	–[c]	2.42

[a]Positive values signify a direction negative in RA.
[b]4σ clipping used for these values.
[c]σ clipping not possible due to broad distribution of results.

5.1 Motion of the disc

Fig. 3 (left-hand panel) shows that in the observed data, the emission in the ring region has shifted at a rate of 0.6 arcsec per year to the right (negative in RA) when tracked from the 1997–1998 to the 2000–2002 epoch. Greaves et al. (2005) argued that at least some of the disc features are tracking with the proper motion of the star, i.e. 1.0 arcsec yr^{-1} to the right. The fact that the net motion measured is smaller may be explained by the presence of stationary background features behind the ring, which by themselves would produce a minimum in the χ^2 curve at 0 arcsec per year. A result intermediate between 0 and 1 arcsec yr^{-1} thus indicates a mixture of tracking and stationary features. The net value of ≈0.6 arcsec yr^{-1} suggests that the majority of features in the ring region are truly associated with ϵ Eridani.

The simulations (Table 1) reproduce this result closely. An input proper motion of 1 arcsec yr^{-1} is recovered as on average ≈0.7 arcsec yr^{-1} of net motion (with little dependence on any assumed ring rotation). Thus, the stationary galaxies do in fact reduce the net motion measured in the same sense as inferred in the real data. The standard deviation of the proper motion solutions is approximately ±0.4 arcsec yr^{-1}. Thus, the real-data solution of 0.6 arcsec yr^{-1}, differing by only ≈0.1 arcsec yr^{-1} from the typical simulation result, is well within the scatter.

Further tests confirmed the validity of the simulations. When the observed data were corrected for the proper motion of the star, the solution obtained was 0.4 arcsec per year to the left (positive in RA). This is a measure of the amount of emission that is fixed in the sky and so moving to the left in the co-ordinate frame of the star. This is the value expected, as the difference between the 1 arcsec yr^{-1} if all the emission moved with the star and the 0.6 arcsec actually measured. A set of simulations was also performed to check that a non-moving disc returned the correct result of 0 arcsec per year. The measured mean was very close to zero (Table 1) with a standard deviation of ±0.25 arcsec yr^{-1}. This is a measure of the fluctuations that can occur due to random noise and chopping on to background galaxies; it is somewhat smaller than the ≈0.4 arcsec obtained in the more complex cases with both stationary and moving flux contributions. Finally, we verified that the small 'ringing' effect seen in the curves in Fig. 3 does not affect the position of the minimum in the χ^2 curves. This ringing arises from a small jump at integer values, apparently in the bilinear interpolation of the 'SLIDE' task in KAPPA. Plotting the curves using only integer values changed the average motions recovered by only ∼0.01 arcsec.

5.2 Rotation of the disc

The χ^2 fit between the observed 1997–1998 and 2000–2002 data sets (corrected for proper motion) shows a rotation of $\approx 2\overset{\circ}{.}75$ per year counterclockwise (see Fig. 3, right-hand panel). This is in the same direction as but somewhat larger than the rotation of $\sim 1\overset{\circ}{.}5$ suggested by Greaves et al. (2005). It is also larger than the rotation rate of $0\overset{\circ}{.}7$–$1\overset{\circ}{.}3$ per year predicted by Ozernoy et al. (2000) and Quillen & Thorndike (2002), assuming dust is trapped in resonances with a planet at ≈40–60 au from the star.

The simulated data are used as a guide to what rotation rates can be confirmed or ruled out. In the simulation results (Table 1), the χ^2 fit results from sets of 100 image-pairs showed that the rotations obtained were approximately Gaussian distributed, for the cases where the rotation rate was 0°, 1° and 2° per year. There were, however, a few spurious results which involved an unphysical disc feature rotation rate (total rotations of $>50°$). These results occurred when a bright clump was randomly generated by a combination of noise and background galaxies and fortuitously positioned in the dust ring to give a deeper minimum in the χ^2 curve corresponding to a large rotation angle. These outcomes ($\leqslant 5$ per set of 100 simulations) did not fit into the Gaussian distribution and were removed by clipping at the 5σ level. After removing these points, the sample standard deviation was typically $\sim 1\overset{\circ}{.}5$ of rotation per year. For rotation rates of 4° and 10° per year, the rotations obtained followed a broader distribution, and so no reliable measure of the rotation was obtained.

The true rotation rate is generally not recovered in the simulations, with an average annual rotation measured generally about half of the input rotation. This can be understood as the effect of the stationary galaxies, which will introduce a bias towards a solution of zero. (When no rotation is input, a solution close to zero is in fact recovered.) Only simulations in roughly the -1σ tails of the distributions recover the true input rotation rate (Table 1). There is therefore a moderate probability that the rate measured in the real data, of $\approx 2\overset{\circ}{.}75$ per year, is actually an underestimate for the true value.

Table 1 shows that for the simulated data with no rotation of the foreground, the sample standard deviation was $1\overset{\circ}{.}58$ per year. As the measured rotation was $2\overset{\circ}{.}75$ per year, this means that the null hypothesis (zero or very slow ring rotation) is ruled out at the $\approx 2\sigma$ level. However, the actual rotation rate cannot be extracted from comparison with the simulations as the results overlap; that is, the standard deviations are wider than the changes in mean value between sets with different input rotation rates. Some estimate can be made of how plausible a measured rotation rate of $2\overset{\circ}{.}75$ anticlockwise is within each simulation set. We find that the probability of measuring at least this large a counterclockwise rotation is 10–25 per cent for rotation rates of 1°–4° per year.

Tests were made to see if any further observational constraints reduced the simulation parameter space. In the real data, the brightest signal is 10 mJy within one beam. Galaxies brighter than this within the 70 arcsec box are predicted to occur in only ≈5 per cent of the simulations. Eliminating these might reduce the tendency towards solutions of zero rotation, but in fact an increase of approximately 20 per cent was the largest change to any recovered rotation rate when this was done.

We also verified that small defects seen in the curves about zero probably arising from interpolation in the rotation process did not significantly change the results. Removal of the defects only changed the rotation rate recovered of the non-moving non-rotating case and only by $\sim 0\overset{\circ}{.}001$ per year and the associated standard deviation by only $\sim 0\overset{\circ}{.}004$ per year.

5.3 Future observations

Table 2 shows the results for the simulated data sets with a third image with no noise included. This is intended to reflect observations that could be made with SCUBA-2 at 850 μm in 2007, with noise that is negligible compared to random background galaxies. Chopping was re-introduced to allow matching of SCUBA and SCUBA-2 images, although testing showed that this only significantly reduced the random fluctuations in the minima in the 4° and 10° per year cases. The χ^2 minima were found by comparing this simulated SCUBA-2 data set with the two simulated SCUBA predecessors, as described above. The projected 10-yr timeline should refine the solutions for the disc motions, and so the annual errors are expected to be reduced.

The proper motion is now recovered at similar mean values to before (≈0.7 arcsec per year) but with lower standard deviations. The errors of $\approx \pm 0.25$ arcsec yr^{-1} are similar to the SCUBA-only non-moving simulation, suggesting this is a limit set by the fluctuations within the two SCUBA data sets from 1997–1998 and 2000–2002. The input rotation is not recovered more reliably than before but the dispersion of the results is smaller, significantly so in the cases of up to 2° yr^{-1} rotation. The number of doubtful results with very large rotations is also reduced (Table 2). However, the distributions of rotation values still overlap between different input rates, and so addition of a third-epoch SCUBA-2 image would not uniquely identify the true rotation rate. In fact, eliminating noise by comparing two hypothetical future SCUBA-2 observations, with mid-points 4 yr apart, still did not resolve this ambiguity. We conclude that χ^2

Table 2. Proper motion shifts and rotations recovered from χ^2 fitting of six simulated data sets including the SCUBA frames of Table 1 and a SCUBA-2 image to be obtained in 2007 (for which no noise is included).

Simulation set no.	Simulated motion[a] (arcsec yr^{-1})	Average motion (arcsec yr^{-1})	Motion σ (arcsec yr^{-1})	Simulated rotation (° yr^{-1})	Average rotation (° yr^{-1})	Rotation σ (° yr^{-1})	5σ Clipping results (no. excluded)	Average min χ^2 value
1	0	0.00	±0.07	0	−0.05	±0.26	0	2.05
2	+1	0.81	±0.21	0	0.05	±0.64	0	3.07
3	+1	0.78	±0.22	−1	−0.52	±0.68	0	3.19
4	+1	0.75	±0.22	−2	−1.04	±1.08	1	3.11
5	+1	0.76	±0.25	−4	−2.48	±1.79	1	3.44
6	+1	0.76	±0.25	−10	−3.70	±6.00	–[b]	4.52

[a]Positive values signify a direction negative in RA.
[b]σ clipping not possible due to broad distribution of results.

fitting alone cannot identify an orbital period; the paradox inherent in trying to fit both moving and non-moving components with one rotation rate is likely to be responsible.

With the inclusion of the SCUBA-2 epoch, the case of no rotation could be ruled out at the $\approx 4\sigma$ level. The average rotation rate recovered was $+0\overset{\circ}{.}05$ per year with a sample standard deviation $\pm 0\overset{\circ}{.}64$. Hence, if the rotation rate of $-2\overset{\circ}{.}75$ per year estimated from the present data was to persist, this would be around the -4σ bound of this simulation. Further, a rotation rate of $\geqslant 1^{\circ}\,\mathrm{yr}^{-1}$ would be confirmed at around the 3σ level: that is, a continuing measurement of $-2\overset{\circ}{.}75$ per year would be just outside the -3σ tail of the simulation with an input rate of $1^{\circ}\,\mathrm{yr}^{-1}$. This would support clumps orbiting faster than the Keplerian rate at $\approx$65 au radius, which is $0\overset{\circ}{.}65$ per year for a 0.9 $\mathrm{M}_{\odot}$ star.

It may also be possible to observe at 450 μm with SCUBA-2, and the improved resolution of 8 arcsec at this wavelength may allow the rotation to be constrained more accurately. This would require two epochs of SCUBA-2 data a few years apart, and also a better knowledge of the galaxy counts at 450 μm.

6 CONCLUSIONS

We have identified a motion of the ϵ Eridani disc consistent with features tracking in the same direction as the proper motion of the star. The best-fitting proper motion $\mu = 0.6 \pm 0.4$ arcsec per year is most probably less than the star's proper motion of 1 arcsec per year, confirming that some of the features in the vicinity of the disc are likely to be background galaxies. The measured rotation rate of $2\overset{\circ}{.}75$ per year counterclockwise is in the same direction but nearly twice as large as that suggested by Greaves et al. (2005); it could also be an underestimate as stationary galaxies tend to bias the rotation solution below the real amplitude. Comparisons with simulated data show that the measured rotation is significant at the $\sim 2\sigma$ level, and a future image with SCUBA-2 in 2007 could rule out no or very slow rotation at the $\sim 4\sigma$ level. The technique of χ^2 fitting is inherently limited by trying to find one solution that fits both stationary galaxies and moving ring features, hence a method that identifies individual clumps or a method capable of using the proper motion to distinguish the foreground and background images will be needed to measure the true rotation rate.

Radial velocity detections of a planet are restricted to finding planets out to only a few au from the star. In the case of ϵ Eridani, finding a planet out to tens of au via radial velocity measurements will be extremely difficult since the period of the planet is deduced to be >100 yr, and the magnitude of the Doppler wobble is reduced by the nearly face-on inclination ($\sim 25^{\circ}$) of the disc. However, this viewing angle also means that ϵ Eridani provides a unique opportunity to track the motion of the substructure within the disc. This is the first ever analysis attempting to track clumps rotating in a dusty disc. Future observations with SCUBA-2 can confirm the rotation of clumps in resonance with a planet at tens of au, while imaging with submillimetre interferometers such as the Submillimeter Array (SMA) and the Atacama Large Millimeter Array (ALMA) could radically shorten the time-scale to identify such motions.

ACKNOWLEDGMENTS

CJP would like to thank Paul Clark and Clare Dobbs for helping with Latex questions. The JCMT is operated by the Joint Astronomy Centre, on behalf of the UK Particle Physics and Astronomy Research Council, the Netherlands Organisation for Pure Research and the National Research Council of Canada.

REFERENCES

Archibald E. N. et al., 2002, MNRAS, 336, 1
Audley M. D. et al., 2004, SPIE, 5498, 63
Aumann H. H., 1988, AJ, 96, 1415
Aumann H. H. et al., 1984, ApJ, 278, L23
Barnard V. E., Vielva P., Pierce-Price D. P. I., Blain A. W., Barreiro R. B., Richer J. S., Qualtrough C., 2004, MNRAS, 352, 961
Beichman C. A. et al., 2005, ApJ, 622, 1160
Bertin E., Arnouts S., 1996, A&AS, 117, 393
Currie M. J., Berry D. S., 2004, Starlink User Note 95.28
Di Folco E., Thévenin F., Kervella P., Domiciano de Souza A., Coudé du Foresto V., Ségransan D., Morel P., 2004, A&A, 426, 601
Dominik C., Laureijs R. J., Jourdain de Muizon M., Habing H. J., 1998, A&A, 329, L53
ESA, 1997, The Hipparcos and Tycho Catalogues, ESA SP-1200
Gomes R., 2003, Icar, 161, 404
Greaves J. S. et al., 1998, ApJ, 506, L133
Greaves J. S., Holland W. S., Jayawardhana R., Wyatt M. C., Dent W. R. F., 2004, MNRAS, 348, 1097
Greaves et al., 2005, ApJ, 619, L187
Hatzes A. P. et al., 2000, ApJ, 544, L145
Holland W. S. et al., 1998, Nat, 392, 788
Holland W. S., Duncan W., Kelly B. D., Irwin K. D., Walton A. J., Ade P. A. R., Robson E. I., 2003, SPIE, 4855, 1
Levison H. F., Morbidelli A., 2003, Nat, 426, 419
Macintosh B. A., Becklin E. E., Kaisler D., Konopacky Q., Zuckerman B., 2003, ApJ, 594, 538
Malhotra R., 1995, AJ, 110, 420
Ozernoy L. M., Gorkavyi N. N., Mather J. C., Taidakova T. A., 2000, ApJ, 537, L147
Proffitt C. R. et al., 2004, ApJ, 612, 481
Quillen A. C., Thorndike S., 2002, ApJ, 578, L149
Schutz O., Nielbock N., Wolf S., Henning Th., Els S., 2004, A&A, 414, L9
Song I., Caillault J.-P., Barrado y Navascués D., Stauffer J. R., Randich S., 2000, ApJ, 533, L41
Williams J. P., de Geus E. J., Blitz L., 1994, ApJ, 428, 693
Wyatt M. C., Dent W. R. F., 2002, MNRAS, 334, 589
Wyatt M. C., Dermott S. F., Telesco C. M., Fisher R. S., Grogan K., Holmes E. K., Pina R. K., 1999, ApJ, 527, 918
Wyatt M. C., Dent W. R. F., Greaves J. S., 2003, MNRAS, 342, 876

This paper has been typeset from a TEX/LATEX file prepared by the author.